TRENDS IN TROPICAL CIRCULATION OVER THE PACIFIC DURING THE LAST DECADE.

Alexander Ruzmaikin and Hartmut H. Aumann

Jet Propulsion Laboratory, California Institute of Technology,
4800 Oak Grove Drive, Pasadena, CA 91109, USA;
emails: Alexander.Ruzmaikin@jpl.nasa.gov; Hartmut H. Aumann@jpl.nasa.gov

ABSTRACT

The Aqua spacecraft decadal time span generated a vast volume of data that can be used for climate change studies. Here we use these data to investigate the tropical circulation response to global warming during the last decade. We use the Atmospheric Infrared Sounder (AIRS), Advance Microwave Sounding Unit (AMSU) and the Advanced Microwave Scanning Radiometer for EOS (AMSR-E) data obtained on Aqua spacecraft to determine the trends in the surface and mid-troposphere temperatures, as well as trends in cloudiness, Outgoing Longwave Radiation (OLR) and precipitation over the West and East Pacific in 2002-2011. The Aqua instruments deliver accurate, simultaneous measurements of the state of the atmosphere twice per day. We find that the tropical (Walker) circulation over Pacific Ocean has been accelerating during this last decade.

Index Terms— IR and Microwave Sounders, Tropical Circulation, Trends

1. INTRODUCTION

Recent climate studies indicate a change in the tropical circulation. Early studies suggested that global warming would reduce the strength of the mean tropical atmospheric circulation [*Knutson and Manabe,*1995]. An essential part of the tropical circulation is a large-scale east-west overturning air circulation across the equatorial Pacific driven by convection in the West Pacific and by subsidence to the East Pacific, called the Walker circulation. More recent studies consistent with climate model simulations driven by anthropogenic forcing indicate that the evolution of the Indo-Pacific gradient of the sea level pressure in the last century indicates a weakening of the Walker circulation [*Vecchi et al,*2006]. This weakening leads to persistent sea level rise in East Pacific and dominance of the El Niño with serious global climate consequences. Analyses of data products comprising the Global Precipitation Climatology Project (1979-2007) and the International Satellite Cloud Climatology Project (1984-2007) show the intensification of tropical precipitation in the rising regions of the Walker and Hadley circulations and weakening of the precipitation over the sinking regions of the associated overturning circulation [*Zhou et al,*2011]. This evolution of the precipitation is not what is expected from the Clausius-Clapeyron law, which would indicate a relative decrease of moisture ascending in the West Pacific. Since the Walker circulation is closely related to the El Niño and monsoons over adjacent continents, and variations in its intensity affect global climate it is important to further investigate its variability.

Here we use the Atmospheric Infrared Sounder (AIRS) and the Advance Microwave Sounding Unit (AMSU) data obtained on Aqua spacecraft to determine the trends in the surface and mid-troposphere temperatures, as well as trends in cloudiness and the Outgoing Longwave Radiation (OLR) over the West and East Pacific in 2002-2011. The AIRS and AMSU deliver accurate, simultaneous measurements of the atmosphere near the surface and in the mid-troposphere [*Aumann et al,*2004]. These data are complemented by the use of precipitation data obtained by the AMSR-E instrument on Aqua spacecraft [*Imaoka et al,*2002]. The AMSR-E (Advanced Microwave Scanning Radiometer for EOS) is a twelve-channel, six-frequency, total power passive-microwave radiometer system. AMSR-E data are produced by Remote Sensing Systems and sponsored by the NASA Earth Science MEaSUREs DISCOVER Project and the AMSR-E Science Team. The data provide twice per day coverage of the Earth's atmosphere from the sea level to the stratosphere. All-sky (including cloudy) day and night data are analyzed. To investigate the change in the sea level pressure we use the data from National Centers of Environmental Predictions (NCEP) for the same decade.

2. THE DATA AND METHODS OF TREND EVALUATION

We examine the L1B AIRS ACDS data for OLR, DCC, BT and SST during the 9-year long time period (September 1, 2002 to August 31, 2011). AIRS generates four million spectra each day by scanning ±49 degrees cross-track with the field of view of 1.1^o in diameter (13.5 km at nadir). About 10% of these data (300,000 spectra each day) are within 3 degree of nadir. About 2% of the near nadir spectra, typically 6500, are selected randomly each day and saved in the AIRS Calibration Data Subset, available since the start of the

AIRS routine operations phase in September 2002. Half of the daily samples come from the 1:30 AM local time overpasses, referred to as “night”, the other half come from the 1:30 PM overpasses, referred to as “day”. Each random spectrum saved in the ACDS is associated with the surface temperature, a land fraction, an infrared (spatial coherence based) clear flag and a reflected light measurement. The surface temperature is obtained from the NOAA Global Forecast System [*Iredell and Caplan,*1995] and interpolated in space and time to the match the sample times and positions. The OLR for each footprint was derived directly from AIRS L1B spectral radiances using regression trained on L2 V6 footprints associated with high quality retrievals. The uncertainty in the OLR is about 2 W/m2, which we treat as a 1% multiplicative error, i.e. the larger the OLR, the larger the error [*Aumann et al,*2012].

We define the West Pacific by the latitudes 30^oS-30^oN and by the longitudes $120^o - 170^o$, and the East Pacific in the same the latitude range by the longitudes $170^o - 250^o$. The data for precipitation from the AMSR-E instrument are available at www.remss.com. We use here the updated version-7 of the data. In addition to the Aqua data we use sea level pressure (SLP) data from the NCEP Reanalysis.

Trends are first calculated as least-squared linear fits with errors estimated using the bootstrap procedure [*Chernick,*1999]. Then we check the value and significance of the trends using the Mann-Kendal test at 95% significance level and the residuals obtained by of the Empirical Decomposition Method [*Huang and Wu,*2008]. The Empirical Mode Decomposition is a non-linear, adaptive data analysis method designed to separate the noise, natural variability and trend in time series.

3. TRENDS

Vecchi et al [2006] analyzed the sea level pressure trends in the Pacific Ocean for the time period 1854-2003 and have found a long-term negative trend in the East-West Pacific gradient. The method used by these authors is based on the relationship between the zonal wind and the pressure gradient in equatorial region:

r

$$\rho abs(\mathbf{u})\mathbf{u}dax \propto -[\mathbf{P}(\mathbf{East}) - \mathbf{P}(\mathbf{West})], \qquad (1)$$

where P is the pressure in the air boundary layer (sea level pressure, SLP), u is the eastward wind and the integral is taken eastward along the equator [*Clarke and Lebedev,*1996]. The negative trend in the pressure gradient indicates a weakening of the Walker circulation. The ensemble-mean GCM experiments revealed that the weakening is caused by anthropogenic (CO_2 forcing [*Vecchi et al,*2006].

FIgure 1 shows the sea level pressure trends for the West and East Pacific in the last decade. We see a small negative trend in the West but the SLP in the East has a much stronger positive trend. According to Eq. (1) this trend implies the acceleration of the westward trade wind and thus the acceleration of the Walker circulation. To further test the difference in the trends we decompose the West and East Pacific data sets into Empirical Modes (Figure 2). The residual, non-oscillating modes show the contrasting trends for the West and East Pacific in agreement with the linear fits directly to the data used in Figure 1.

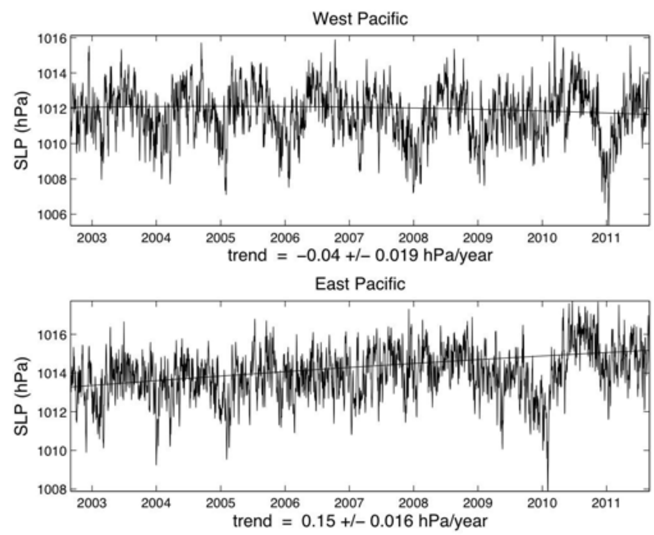

Fig. 1. Trends in Sea level pressure for the West Pacific (upper panel) and for the East Pacific (lower panel). The trends are determined by the least square fits and listed under each panel. In parenthesis we show the trend errors at 2 level, which are found using the bootstrap procedure applied to each data set.

Figure 3 shows data time series and trends over the West and East Pacific for other variables. We see that the temperature trend in SST and mid-troposphere over the East Pacific is larger than the trend over the West Pacific. There is also the West-East difference in the DCC trends and the East-West difference of the OLR trends: a clearer East Pacific generates increasing longwave outputs.

The trends in precipitation are shown in Figure 4. We see a significant negative trend in the West Pacific but insignificant (or no) trend in the East Pacific. There is a strong peak in the last 2010-2011 year, but the trend remains insignificant even if we cut off the data that include the peak and fit the trend to the time period 2002-2009.

4. DISCUSSION

Our analysis of the data obtained by instruments on Aqua satellite and data from NCEP Reanalysis shows that the Walker Circulation has been accelerating during the last 9 years. The East-West Sea Level gradient is accelerating in 2002-2011. Temperature trends in SST and mid-troposphere over the East Pacific are larger than the trends over the West

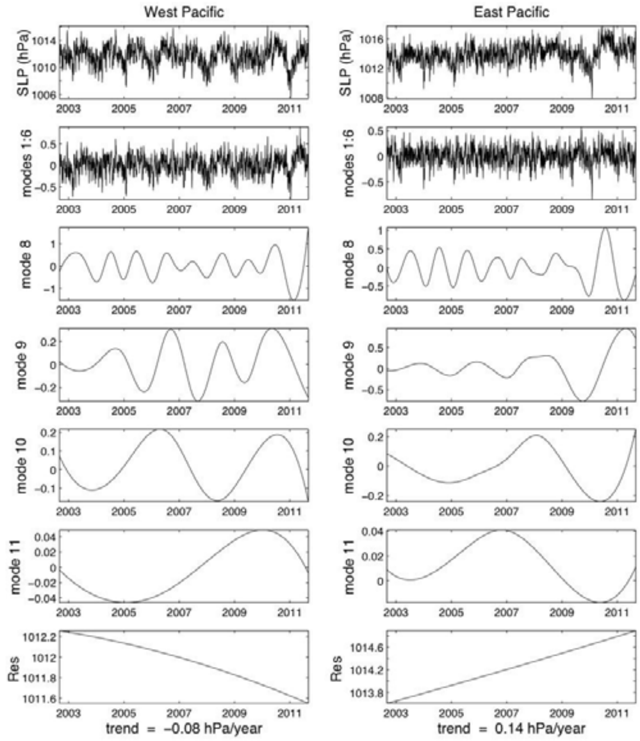

Fig. 2. Empirical Mode Decompositions of the sea level pressure for the West Pacific (left panels) and for the East Pacific (right panels). The upper panels plot the data. The second panels combine the first six (noisy) modes. The residuals (last panels) show the trends.

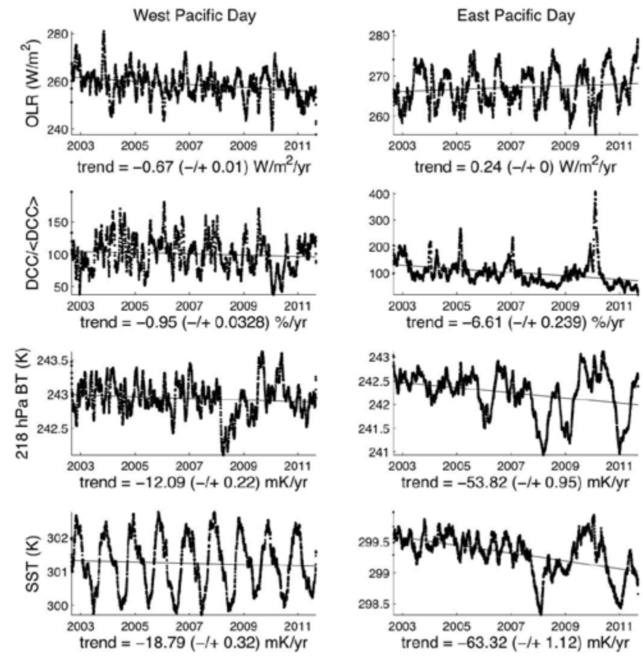

Fig. 3. Trends in SST, free troposphere (364 hPa), Deep Convective Clouds (DCC), and OLR for nine years of data from Aqua satellite. The results are shown for ascending (day) orbits, similar trends are obtained for descending orbits. The left columns refer to the West Pacific; the right columns refer to the East Pacific. The trends are determined by the least square fits and listed under each panel. In parenthesis we show the trend errors at 2 level, which are found using the bootstrap procedure applied to each data set.

Pacific. There was a significant West-East difference in the DCC trends, also reflected in different OLR trends: a clearer East Pacific generates increasing longwave outputs. According to the Clausius-Clapeyron relation one should expect a relative increase of moisture ascending in the West Pacific. However we see only a slight negative trend in the precipitation over the West Pacific and no significant trend over the East Pacific. A possible explanation can be related to the fact that we use data covering extended spatial regions the precipitation in which it is mainly determined by heavy (extreme) rains. The evolution of the rainfall extreme precipitation in response to the global temperature changes does not follow the Clausius-Clapeyron law. The heavy rain events increase during warm periods and decrease during cold periods [**?**]. If mostly the heavy rains determine the precipitation over the West Pacific then the negative trend (Figure 4) is consistent with the SST cooling (Figure 3). It is consistent with the trend difference in Deep Convective Clouds, which represent the extreme heavy rains.

To put the result of our data analysis into the context of causes of climate change we take into consideration the forcing and natural variability that took place in the Pacific during the 9-year time span under consideration. The Pacific Decadal Oscillation mostly affects the North Pacific and may be excluded. The global trend due to anthropogenic forcing on decadal scale was lower than in the previous decade. Solomon et al. [2010] found a 10% decrease in stratospheric water vapor concentration in 2000-2009 and indicated that this decrease may slow the rate of increase in global surface temperature by about 25% compared to that that would have occurred due to greenhouse gases. However it remains unclear whether the 2000-2009 decrease in stratospheric water vapor represents a water vapor feedback to anthropogenic global warming or is caused by some other forcing.

The most probable cause of the observed decadal change is the variability of solar irradiance. [*Haigh and Blackburn*2006] suggested a dynamical response of the troposphere to enhanced solar UV and the induced ozone change in the stratosphere via reducing wind speed and broadening the Hadley circulation cell. Another possible mechanism is the increase of solar irradiance at maxima of solar activity that produces greater energy input to the ocean surface in cloud-free areas of the subtropics, evaporating more moisture, and that

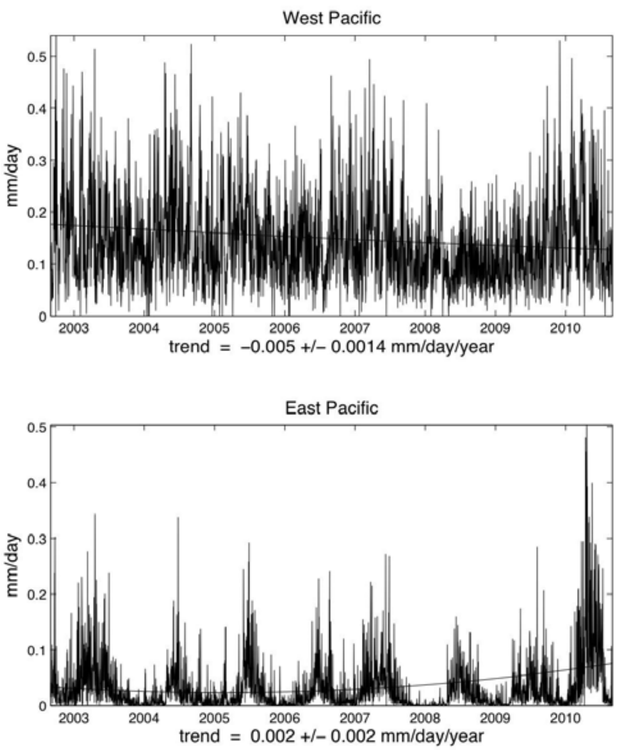

Fig. 4. Trends in precipitation for the West and East Pacific. The West has a small significant negative trends but the trend in the East is significant.

moisture is carried by the trade winds to the convergence zones where more precipitation occurs [*Meehl et al.*(2009)]. Thus intensified precipitation produces greater equatorial ocean upwelling and lower equatorial SSTs in the eastern Pacific. We suggest that the current cooling of the Tropical Pacific Ocean was consistent with the strong decline of solar activity over the time period under consideration, which included the declining phase of the 23rd solar cycle. We have found a negative trend (-0.2K/year, with 95% statistical confidence) in Tropical Pacific SST during the same time period [*Ruzmaikin and Aumann,*2012]. The declining phase of solar cycle 23 approximately covers the time period investigated by Solomon et al. [2010], the -0.2 K/year temperature trend at sea level means that during years of the declining phase of this cycle the temperature dropped on average by about 1.5K.

5. ACKNOWLEDGMENTS

The work was performed at the Jet Propulsion Laboratory, California Institute of Technology under a contract with the National Aeronautics and Space Administration. We acknowledge the use of the Aqua and NCEP Reanalysis data.

6. REFERENCES

Allan, R. P. and B. Soden, Atmospheric warming and the amplification of precipitation extremes, Science, 321, 1481–1484, 2008.

Aumann, H. H., D. Gregorich, S. Gaiser and M. T. Chahine, Application of Atmospheric Infrared Sounder data to climate research, Proc. SPIE, 5570, 202–208, 2004.

Aumann, H. H., A. Ruzmaikin and A. Behrangi, On the surface temperature sensitivity of the reflected shortwave, outgoing longwave and net incident radiation, J. Clim. (in press), 2012.

Chernick, M. R., Bootstrap Methods: A Practitioner's Guide, Wiley Series in Probability and Statistics, 1999.

Clarke, A. J. and A. Lebedev, Long-term changes in equatorial Pacific trade winds. J. Clim. 9, 1020–1029, 1996.

Haigh J. and W. Blackburn, Solar influence on dynamical coupling between the stratosphere and troposphere, Space Sci. Rev. 125, 331–344,doi:10.1007/s11214-006-9067-0, 2006.

Huang, N. E., and Z. Wu, A review on Hilbert-Huang transform: Method and its applications to geophysical studies, Rev. Geophys., 46, 1–23, 2008.

Imaoka, K., Sezai, T., Takeshima, T., Kawanishi, T. and A. Shibata: Instrument characteristics and calibration of AMSR and AMSR-E. Proc. IGARSS 2002, 2002.

Iredell, M., and P. Caplan, Four-time daily runs of the AVN Model, National Weather Service, Tech.Proc.Bull 442, www.nco.ncep.noaa.gov/pmb/products/gfs/, 1997.

Knutson, T. R. and S. Manabe, Time-mean response over the tropical Pacific to increased CO2 in a coupled ocean-atmosphere model. J. Clim. 8, 2181–2199, 1995.

Meehl, G. A., J. M. Arblaster, K. Matthes, F. Sassi, H. van Loon, Amplifying the Pacific climate system response to a small 11-year solar cycle forcing, Science, 235,114–118, 2009.

Ruzmaikin, A. and H. H. Aumann, Decadal variability of tropical Pacific temperature in relation to solar cycles, Advances in Space Research 49, 572-578, 2012.

Vecchi, G. A., B. J. Soden, A. T. Wittenberg, I. M. Held, A. Leetmaa, and M. J. Harrison, Weakening of tropical Pacific atmospheric circulation due to anthropogenic forcing, Nature, 441, 73–76, doi:10.1038, 2006.

Zhou, Y. P., K.M. Xu, Y. C. Sud, and A. K. Betts, Recent trends of the tropical hydrological cycle inferred from Global Precipitation Climatology Project and International Satellite Cloud Climatology Project data, J. Geophys. Res., 116, D09101–D09116, doi:10.1029/2010JD015197, 2011.